Technical Report: A Study of Pathloss and Shadow Fading Models for mmWaves

Victor Croisfelt Rodrigues and Taufik Abrão

***Abstract*—The possibility to use the available spectrum at the millimeter wave (mmWave) range comes to be a great candidate to support the performance demands expected for the fifth generation (5G) of wireless communications. However, mmWave channels are dissimilar to the wider-known propagation phenomenology of the centimeter waves (cmWave), making it necessary a proper physical characterization of such links. Motivated by these facts, this work studies some models of large/medium-scale propagation effects for radios operating at mmWave frequencies. This study is based on measurements campaigns available in literature. The discussions rely on line-of-sight (LoS) probability, large-scale pathloss (PL) and shadow fading (SF) designs. Specific model parameters for urban macro cellular (UMa) environments at a frequency of 28 GHz are analyzed.**

I. Introduction

The wireless connectivity has established as a crucial constituent of the contemporaneous society, in such a way that itself stimulates new demands of services and applications. To meet these requirements, researchers are spurred to develop high-speed and reliable communications for the 5G of cellular networks. Although, telecommunications systems are profoundly impacted by its own wireless medium, due to time-varying impediments such as noise, interference, and propagation effects. In this way, one can observe that the development of bandwidth-efficient and high performance wireless technologies are extremely associated with the propagation environment. Being evident that the study of its phenomenology is fundamental to aid the design of wireless networks.

Nowadays, most of the terrestrial wireless communications commonly operate in the frequency range of several hundreds MHz to a few GHz [1], which corresponds to the microwave frequencies or, looking at the wavelength, a wave that has a length of the order of centimeters, the centimeter waves (cmWave). This beachfront spectrum is exhaustively employed on many applications, as a result of its favorable propagation qualities and the knowledge of a solid radio hardware.

The 5G of cellular technology is goaling to support an enhancement of one thousand times in spectral efficiency (SE) and one of the conventional manners to provide this is to enlarge the frequency bandwidth allocated for the wireless communications. However, the beachfront spectrum has come to be entirely occupied by a diversity of applications, hindering the exploitation of wider bandwidth to this end. Fortunately, an enormous amount of available spectrum do exist at mmWave range that extends from 30-300 GHz and at 20-30 GHz frequencies, where the latter extent is not considered as mmWave, but it is plausible to be utilized as well [1]. Since they are easily obstructed by objects found within the environment, even by the human body, those frequencies are entailed with short-range applications. Thus, the study of channel propagation models is placed as an important prerequisite to design wireless system employing those unused frequency ranges.

Victor Croisfelt Rodrigues is with University of São Paulo, São Paulo (USP), Brazil (e-mail: victorcroisfelt@gmail.com). Taufik Abrão is with State University of Londrina (UEL), Londrina - PR, Brazil (e-mail: taufik@uel.br).

Many researches present channel sounder measurements at mmWave and study their behavior based on different pathloss (PL) and shadow fading (SF) models. Normally, these models are empirically obtained. For instance, the authors in [2] offers a lot of fitting parameters for LoS (line-of-sight) probability, and PL and SF models based on measurements conducted at different frequencies collected within a UMa environment. The parameters are obtained by utilizing the minimum mean square error (MMSE) fitting approach. We emphasize that the data collected in [2] is from a radio operating at a frequency of 28 GHz. This frequency is also adopted in [3], where fitting parameters are shown for PL and SF models within a UMa environment. In addition to that, this paper discusses two typical problems of accuracy errors obtained when using the least-square (LS) fitting approach (or other fitting approaches): the bias and censored data.

II. Urban Macro Cellular Scenario

The UMa scenarios are quite similar in the considered works [2] and [3], where the former was realized at Aalborg University (AAU), whereas the latter at New York University (NYU). Moreover, both areas are comprised of buildings of $20 - 40$ m high, some open areas, vegetation, and streets. Commonly, UMa environments have their base station (BS) located at a height of $20 - 40$ m (rooftop of the highest building). The communication links are likely associated with an outdoor environment, where mobile receiver antennas are typically located at 1.5 m above the ground. The coverage radius is generally at the range of $400 - 600$ m.

III. LoS Probability

Several works conducted empirical measurements to design a model that describes which is the chance that a given channel is in a LoS condition at a specific distance. Intuitively, note that this quantity is very related to the evaluated environment, whose fact hinders obtaining a tight expression to describe a large collection of deployment scenarios. Thereby, some of these models were suitably set to describe such amount, called as LoS probability, being the main ones discussed further on.

$$\mathrm{PL}^{\mathrm{FI}}(d) = \begin{cases} \alpha + 10\beta_1 \log_{10}(d/1\text{ m}), & \text{for } d < d_{\text{break}} \\ \alpha + 10\beta_1 \log_{10}(d_{\text{break}}/1\text{ m}) + 10\beta_2 \log_{10}(d/d_{\text{break}}), & \text{for } d > d_{\text{break}} \end{cases}. \quad (1)$$

The first model is based on the 3GPP 3D channel model [4], although with the presence of some parameters which have to be optimized in a given circumstance. Note that, since the genuine model given by 3GPP does not agree well with mmWave frequencies, as it does for the cmWave range [2], these parameters have to be additionally considered. In addition to that, the authentic model is restricted to an antenna height of 25 m, which is not strictly true under UMa conditions, as already mentioned. Thus, the modified 3GPP 3D LoS probability model is given as:

$$p(d) = \min\left(\frac{d_1}{d}, 1\right)\left(1 - e^{-\frac{d}{d_2}}\right) + e^{-\frac{d}{d_2}}, \quad (2)$$

where d is the distance between a transmitter and a receiver (Tx-Rx), d_1 and d_2 are fitting parameters, i.e., they have to be optimized through the realization of a fitting procedure.

Another expression to model the LoS probability was proposed by the authors in [5] of the NYU as:

$$p(d) = \left(\min\left(\frac{d_1}{d}, 1\right)\left(1 - e^{-\frac{d}{d_2}}\right) + e^{-\frac{d}{d_2}}\right)^2. \quad (3)$$

The above expression is basically given by the squared version of (2), which is argued by the authors in [5] to be more suitable in mmWave scenarios.

At last, a simple model relying exclusively on the effect of an inverse exponential summed with a constant is denoted below [6]. Due to the presented fact, this model is commonly referred to as the *inverse exponential model*.

$$p(d) = \frac{1}{1 + e^{d_1(d - d_2)}}. \quad (4)$$

Note that the three models introduced are dependent on the inverse of an exponential, establishing as a common model that represents the decay of the LoS probability over the increasing of the Tx-Rx distance.

TABLE I
FITTING PARAMETERS FOR LOS PROBABILITY MODELS COLLECTED UNDER A UMA SCENARIO OPERATING AT 28 GHZ [2].

LoS Probability Models	d_1 (m)	d_2 (m)	MSE
3GPP	49	1	0.0135
NYU	0	395	0.0103
Inverse Exponential	0.0054	97	0.0076

Some empirically-obtained parameters and the mean squared error (MSE) are disposed in Table I based on the data collected in [2]. One observes that the inverse exponential model achieves the minor MSE. Besides, Fig. 1 was conceived to support the visualization of the models and the given parameters.

Although the inverse exponential model gives the best MSE, it does not predicts very well the behavior of the data changes.

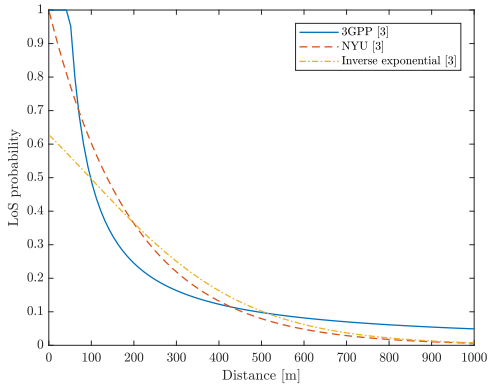

Fig. 1. LoS probability as a function of the Tx-Rx distance considering the three models presented above and the data collected in [2].

Because of this, the authors in [2] presumed that new models for LoS probability has to be studied. Recent works are proposing frequency-dependent LoS probability models.

The LoS and NLoS (non-line-of-sight) PL models have typically different behaviors. The PL can be modeled as a function of the distance as:

$$\mathrm{PL}(d) = p(d)\mathrm{PL}_{\mathrm{LoS}}(d) + (1 - p(d))\mathrm{PL}_{\mathrm{NLoS}}(d), \quad (5)$$

where $\mathrm{PL}_{\mathrm{LoS}}(d)$ and $\mathrm{PL}_{\mathrm{NLoS}}(d)$ represents the PL for LoS and NLoS conditions, successively. Note that the complement of $p(d)$ directly represents the NLoS probability. Thus, one can conclude that the PL at a certain distance is given as the combination of the LoS and NLoS PL models, duly weighted by their probabilities; the same occurs for SF.

IV. PATHLOSS

Intrinsically, the power of a signal radiated by a given transmitter spreads out when this wave travels through the space. This disperse behavior of the wireless channel gives rise to a fundamental phenomenon called as PL, which elementally limits the coverage area and data rates of a communication system through the determination of both signal-to-noise and signal-to-inference ratios [7]. PL is commonly associated with the distance between a transmitter and a receiver, where, as larger the distance is, smaller comes to be the amount of power which reaches the receiver. Another variable attached to this effect is the signal frequency. High frequencies are more obstructed by the environment constituents, further confining more the coverage of communication systems operating in the mmWave range than in cmWave. Therefore, one can deduce that the need for reliable PL models is crucial to hand the design of communication networks adopting either frequencies.

$$\sigma^{\mathrm{FI}}(d) = \begin{cases} a + b_1 \log_{10}(d/1\text{ m}), & \text{for } d < d_{\text{break}} \\ a + b_1 \log_{10}(d_{\text{break}}/1\text{ m}) + b_2 \log_{10}(d/d_{\text{break}}), & \text{for } d > d_{\text{break}} \end{cases}. \tag{6}$$

There are several models to describe PL, being useful to divide them in single-frequency and frequency-agile or multi-frequency models. The latter is applied to cover a wide-range of frequencies. For example, a model that embraces the cmWave and mmWave simultaneously (see [8], for instance). While the single-frequency models stands for mathematical expressions that strive to well fit the design of specific frequency scenarios. This set of models permits the visualization of the problem by exploring different approaches, such as the use of double-slope functions. These are used to describe the change of the PL impact over the distance, achieving minor fitting errors. In fact, the model parameters are obtained through data fitting or ray tracing, where the most common fitting approaches are the LS, the MMSE, or even, the maximum likelihood (ML). Herein, the single-frequency models based on floating intercept (FI) functions will be discussed and supported by illustrative results.

The FI model is based on the classical log-distance power law [7]. It was proposed as a way to reduce the complexity obtained through high-order ray-tracing techniques. The FI model can be defined as:

$$\mathrm{PL}^{\mathrm{FI}}(d) = \alpha + 10\beta \log_{10}(d/1\text{ m}), \tag{7}$$

where α represents the FI parameter. This term consists of a degree of freedom which strive to improve the fitting process, since it can be changed in anyway to better data adjustment. β denotes the single-slope coefficient obtained through the realization of a fitting approach. Furthermore, it is noteworthy to say that α does not rely on a physical characteristic of the PL phenomenology, and hence, it is solely a mathematical tool to improve fitting accuracy.

The dual-slope FI model is defined in (1). Note that a break-point distance is defined as a delimiter between the single and double-slope effects. This distance is called as the break-distance and represented by d_{break}. The dual-slope function strives to mitigate the fitting error at large distances. This is because, at large distances, we have bad measurement resolution and aggravate effect of arbitrariness.

It is known that models based on these fitting procedures ignore certain properties of the measured data. One of these is that typical PL data exist at locations whose density is unevenly distributed over the link distances. This can cause bias in the PL model fitting, favoring distances with more data samples. The authors of [3] shown that typical LS fitting applied over raw data points is inherently biased to give the best fitting to the link distances that happen to have more evaluated points. Another important disregarded aspect is that certain PL values cannot be measured because of the limited hardware sensibility and the noise floor, giving rise to censored measurement data. To alleviate these effects, first, a PL fitting approach with distance-dependent weighing is proposed in [3]. Second, it has been shown that adding censored samples contribute to improve the parameter estimation.

Still relying on [3], the authors demonstrated that PL under LoS condition yields in a better fitting when considering a single-slope PL model and a single-slope distance-dependent SF model. However, a dual-slope for PL and SF is required under NLoS, since the randomness and censored data hinder a good matching between data and modeling.

V. Shadow Fading

The shadow fading stands for the random fluctuations of the received power at a given distance, which stems from reflecting surfaces and scattering objects. Actually, this effect can be also viewed as a correction factor of empirical PL models. Due to the lack of knowledge of the location, size, and dielectric properties of those blocking objects situated in the environment, a statistical model is commonly applied to design the SF. It is well-suited that a log-normal random variable models satisfactorily the SF, as verified by empirical results. This random variable is characterized by a mean μ and a standard deviation σ. The values of μ and σ are also obtained with the aid of channel measurements.

In some environments, σ can be described by a single-slope or even a dual-slope function of the distance as a reflection to the modeling used for PL. Straightforwardly, the standard deviation measured in dB (decibels) can be modeled as a single-slope function as:

$$\sigma^{\mathrm{FI}}(d) = a + b \log_{10}(d/1\text{ m}), \tag{8}$$

where a is the FI parameter and b is the slope. The SF dual-slope equivalent to the presented for PL is given in (6).

VI. Illustrative Example

By associating the models and insights given above, the authors in [3] acquired some values of PL and SF models in LoS and NLoS conditions.

First, the optimal models (OMs) are presented, where the PL and SF for LoS and NLoS conditions are said to be the most favorable, since they reach minor errors. They are modeled as [3]:

$$\begin{aligned} \mathrm{PL}_{\mathrm{LoS}} &= 64.88 + 16.7 \log_{10}(d/1\text{ m}) \\ \sigma_{\mathrm{LoS}} &= -1.20 + 1.54 \log_{10}(d/1\text{ m}) \end{aligned} \tag{10}$$

where the weighting method (b) was chosen, which stands for an equally weight through the distance bins (see [3] for detailed discussion). This picking is motivated by the further consideration of uniform distribution of the user equipments over the coverage area. Notwithstanding, the LoS scenario does not have the consideration of censored data and the FI superscript was omitted from the above equation for ease of exposition.

$$\mathrm{PL}_{\mathrm{NLoS}}(d) = \begin{cases} 83.8 + 17.5\log_{10}(d/1\text{ m}), & \text{for } d < 148.2 \\ 83.8 + 17.5\log_{10}(148.2/1\text{ m}) + 119.0\log_{10}(d/148.2), & \text{for } d > 148.2 \end{cases}$$
$$\sigma_{\mathrm{NLoS}}(d) = \begin{cases} -0.002 + 7.3\log_{10}(d/1\text{ m}), & \text{for } d < 148.2 \\ -0.002 + 7.3\log_{10}(148.2/1\text{ m}) + 27.2\log_{10}(d/148.2), & \text{for } d > 148.2 \end{cases} \quad (9)$$

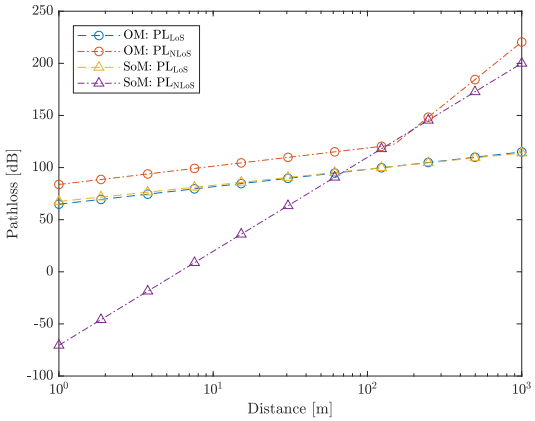

(a) OMs and SoMs PL as a function of the Tx-Rx distance.

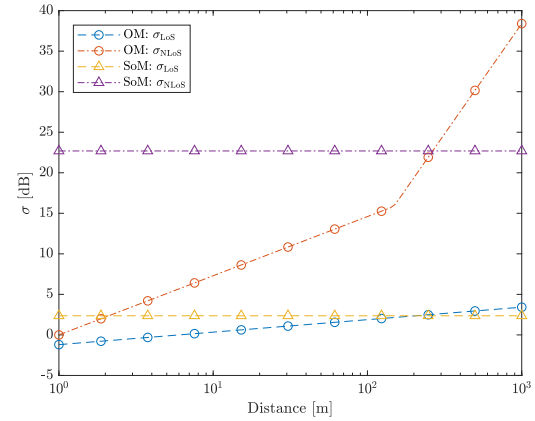

(b) OMs and SoMs standard deviation (σ) of SF as a function of the Tx-Rx distance.

Fig. 2. OMs and SoMs as a function of the Tx-Rx distance; where in (a) the PL models are being evaluated, whereas in (b) the standard deviation model related to SF.

The PL and SF OMs for the NLoS scenario is presented in (9), wherein a censored level of 170 dB is applied and any weighting procedure was done. The latter because of the sufficient complexity generated by the six parameters modeling, jointly with its achievable minor error.

The sub-optimal models (SoMs) accepts a great modeling error and are given as follows:

$$\begin{aligned} \mathrm{PL}_{\mathrm{LoS}} &= 67.48 + 15.5\log_{10}(d/1\text{ m}) \\ \sigma_{\mathrm{LoS}} &= 2.36 \\ \mathrm{PL}_{\mathrm{NLoS}} &= -70.5 + 90.17\log_{10}(d/1\text{ m}) \\ \sigma_{\mathrm{NLoS}} &= 22.69 \end{aligned} \quad (11)$$

where it is considered the weighting method (b) for all data bins and censored data of 170 dB in the NLoS case.

Fig. 2 shows the OMs and SoMs defined in (10), (9) and (11), respectively. Regarding the PL models in Fig. 2a, observe that the OM and SoM PL LoS are comprised of a single-slope function and do not exhibit large differences, as expected from their α and β values. On the other hand, the PL NLoS reveals to be quite dissimilar, since the OM case handles with a dual-slope function, while the SoM a single-slope. Notice the effect in utilize a dual-slope function, where the single-slope is striving to fit the data at long distances since its beginning, which harms the model for short distances. On the other hand, the dual-slope function can divide the fitting procedure in two zones, which guarantees a better match.

The SF models are exhibited in Fig. 2b, where the OMs for LoS and NLoS correspond to a single-slope and a dual-slope function, successively; whereas the SoMs present constant σ in both scenarios.

References

[1] J. G. Andrews, S. Buzzi, W. Choi, S. Hanly, A. Lozano, A. C. K. Soong, and J. C. Zhang, "What Will 5G Be?" *IEEE Journal on Selected Areas in Communications*, vol. 32, no. 6, pp. 1065–1082, 2014. [Online]. Available: http://arxiv.org/abs/1405.2957

[2] S. Sun, T. Thomas, H. C. Rappaport, Theodore S.; Nguyen, I. Kovács, and I. Rodriguez Larrad, "Path Loss, Shadow Fading, and Line-Of-Sight Probability Models for 5G Urban Macro- Cellular Scenarios," *2015 IEEE Globecom Workshops*, 2015.

[3] A. Karttunen, C. Gustafson, A. F. Molisch, R. Wang, S. Hur, J. Zhang, and J. Park, "Path loss models with distance-dependent weighted fitting and estimation of censored path loss data," *IET Microwaves, Antennas & Propagation*, vol. 10, no. 14, pp. 1467–1474, 2016. [Online]. Available: http://digital-library.theiet.org/content/journals/10.1049/iet-map.2016.0042

[4] V. 3GPP TR 36.873, "Study on 3D channel model for LTE (release 12)," Tech. Rep., 2018.

[5] M. K. Samimi, T. S. Rappaport, and G. R. MacCartney, "Probabilistic Omnidirectional Path Loss Models for Millimeter-Wave Outdoor Communications," *IEEE Wireless Communications Letters*, vol. 4, no. 4, pp. 357–360, 2015.

[6] I. Rodriguez, H. C. Nguyen, N. T. K. Jørgensen, T. B. Sørensen, J. Elling, M. B. Gentsch, and P. Mogensen, "Path loss validation for urban micro cell scenarios at 3.5 GHz compared to 1.9 GHz," in *2013 IEEE Global Communications Conference (GLOBECOM)*, 2013, pp. 3942–3947.

[7] A. F. Molisch, *Wireless Communications*. John Wiley & Sons Ltd, 2011.

[8] K. Haneda, N. Omaki, T. Imai, L. Raschkowski, M. Peter, and A. Roivainen, "Frequency-agile pathloss models for urban street canyons," *IEEE Transactions on Antennas and Propagation*, vol. 64, no. 5, pp. 1941–1951, 2016.